

## CALCULATION OF FLICKER PROPAGATION IN PART OF THE SLOVENIAN NETWORK WITH VOLTAGE INTERHARMONICS

Miloš MAKSIĆ

Milan Vidmar Electric Power Research Institute  
Ljubljana, Slovenia  
milos.maksic@eimv.si

Igor PAPIČ

Faculty of electrical engineering, University of Ljubljana  
Ljubljana, Slovenia  
igor.papic@fe.uni-lj.si

### ABSTRACT

The assessment of flicker levels in the Slovenian power network is vital, as flicker is a major power quality concern. The paper shows a method of flicker propagation and summation calculation with network interharmonics on a practical example case of two arc furnaces as major flicker-sources. The example shows flicker propagation in the transmission network and further into the distribution network.

### INTRODUCTION

Three arc furnaces have long been causing significant power quality problems related to flicker in the Slovenian power network [1-5]. All three arc furnaces in steelworks differ in their nominal power ratings and in the short-circuit power to which their arc furnace transformers are connected. According to this and the topology of the network, the voltage fluctuations caused by the intermittent consumption of the furnaces propagate to other network nodes in the high-voltage (HV) network and lastly to consumers connected to medium-voltage (MV) and low-voltage (LV) networks with varying attenuation [1, 6]. These voltage fluctuations cause flicker. Flicker intensity can be determined with flickermeter [7]. Furthermore, these voltage fluctuations are added together and the resulting flicker levels in nodes under the influence of more than one flicker source become even higher.

According to its network operation code, the transmission network system operator must prevent severely high flicker levels in the high-voltage network from reaching the distribution network to which the end-users are connected so that their power quality levels according to standard EN 50160 [8] are not violated. The paper assesses flicker levels in a chosen network node that is influenced by two furnaces whereas the effect of the third furnace and other flicker sources can be neglected. Flicker levels are calculated according to the theory of propagation and summation of voltage interharmonics [2-5].

Furthermore, an additional case study of flicker propagation from the HV to the distribution MV grid is shown.

### STUDIED NETWORK

Figure 1 shows the transmission network under study. A and B in figure 1 denote the two 110 kV nodes to which the arc furnaces with 40 MVA and 36 MVA power ratings,

respectively, are connected. Instantaneous voltages in nodes A, B and Y on their HV and MV levels were measured for a time period of one week. During this time the studied network node Y was affected by voltage fluctuations from either a single or both arc furnaces, depending on their time of operation. The propagation of voltage fluctuations from furnace A to node Y is affected by high short-circuit power from two power sources connected to 400 kV and 220 kV nodes and also from a 94 MVA source connected to a 110 kV node as is shown in figure 1. Furnace B is electrically closer to node Y but is also affected by the operation of a chain of hydro power plants in its vicinity one of which, a 30 MVA plant is shown in figure 1.

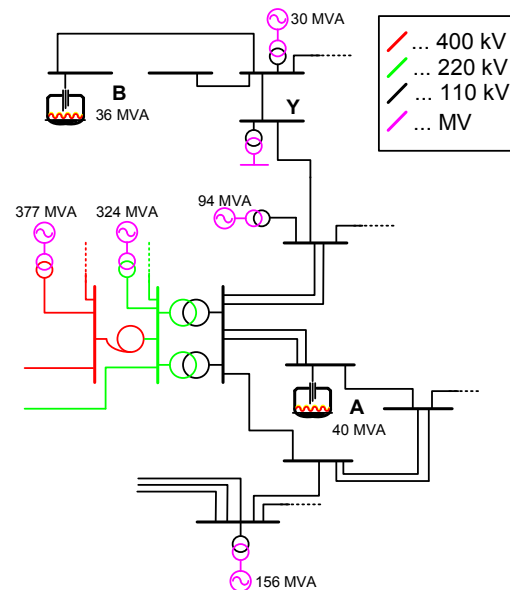


Figure 1. The network under study.

### CALCULATION OF FLICKER PROPAGATION WITH INTERHARMONICS

Voltage interharmonics are calculated from measured instantaneous voltages at the arc furnaces (or other sources of flicker). The propagation of voltage interharmonics in the network is based on network voltage transfer factors  $NVTF$  between the network nodes for each interharmonic component. The network voltage transfer factors between node Y and the source of flicker in a particular node F can be obtained according to:

$$\underline{NVTF}_{Y-F,inth} = \frac{U_{Y,inth}}{U_{F,inth}} = \frac{Z_{th,inth} - Z_{2,inth}}{Z_{2,inth}} \quad (1)$$

for each interharmonic component “inth”, where  $Z_{th}$  represents the Thevenin impedance of node F and  $Z_2$  is the equivalent impedance between nodes F and Y. Figures 2 and 3 show  $NVTF$  amplitudes and phase angles at different frequencies between nodes A and Y and between nodes B and Y, respectively.

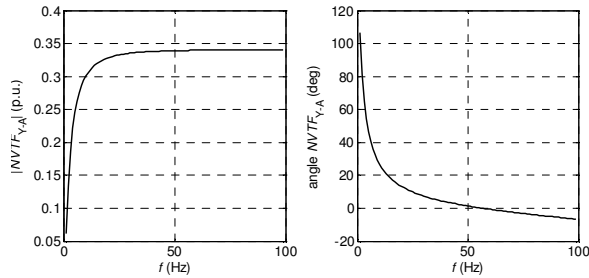


**Figure 2.** Amplitude and phase angle voltage transfer factor between nodes A and Y.

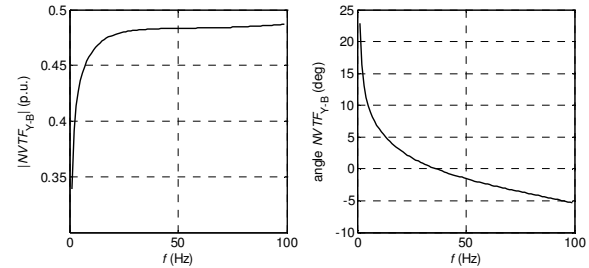


**Figure 3.** Amplitude and phase angle voltage transfer factor between nodes B and Y.

According to figures 2 and 3, the voltage amplitude transfer factor between nodes Y and B is larger compared to the same factor between nodes Y and A. As the furnace B is connected to a node with a smaller short-circuit power this basically means that node Y is mainly influenced by flicker from furnace B.

### Summation of interharmonic components

In cases when both furnaces are in simultaneous operation, the voltage fluctuations (which consequently cause flicker at the end-users in low voltages) from both furnaces propagate to node Y where they add up. The addition of these fluctuations can be achieved with the use of the theory of addition of frequency components. According to the Fourier analysis each signal (e.g. voltage) can be decomposed to a sum of several frequency components:

$$u(t) = U_{DC} + \sum_{i=1}^{N-1} U_i \cos(\omega_i t + \varphi_i), \quad (2)$$

where  $U_i$ ,  $\omega_i$  and  $\varphi_i$  are the amplitude, frequency and phase angle of the  $i$ -th component. The number of frequency components depends on the sampling frequency of the signal and the length of the windowing function. In our case the sampling is 6400 Hz with a rectangular window function of 1-second length. This means that the maximum frequency amounts to 3200 Hz with a  $\Delta f = 1$  Hz resolution. Only a narrow spectrum, mostly between 20 Hz and 80 Hz, determines the flicker [7].

According to this the measured voltages at both arc furnaces can be decomposed according to (2). Next, each frequency interharmonic “inth” component is multiplied by its voltage transfer factor between two nodes to obtain the voltage in node Y (determined by a single source):

$$u_Y = U_{Y,50Hz} + U_{A,inth} NVTF_{Y-A,inth}, \quad (3)$$

$$u_Y = U_{Y,50Hz} + U_{B,inth} NVTF_{Y-B,inth}. \quad (4)$$

The base frequency component  $U_{Y,50Hz}$  can be determined with a load-flow calculation. In cases when both sources are in simultaneous operation, the frequency components add-up:

$$u_Y = U_{Y,50Hz} + \sum_{inth} (U_{A,inth} NVTF_{Y-A,inth} + U_{B,inth} NVTF_{Y-B,inth}). \quad (5)$$

Once  $u_Z$  is obtained the flicker in node Z can be calculated. In cases of flicker propagation through shorter lines a simplified analysis can be made – amplitude transfer factors are set equal for all frequencies  $NVTF = |NVTF_{inth}|$  and the effect of phase angles is neglected. In that case (5) simplifies to:

$$u_Y = U_{Y,50Hz} + u_{A,inth} NVTF_{Y-A} + u_{B,medh} NVTF_{Y-B}. \quad (6)$$

In other cases simplifications in network modelling and in the number of frequency components of  $NVTF$  used can further be made [5].

### CALCULATION OF FLICKER IN THE HV NETWORK DURING SIMULTANEOUS FURNACE OPERATION

Figure 4 shows a 15 minute interval of instantaneous flicker perception  $S(t)$  obtained from voltage measurements in nodes A, B and Y. The contribution of both furnaces in node Y is shown ( $S(t)$  measured in A and B is multiplied with approximate transfer factors between the two nodes and node Y from figures 2 and 3) as well as a cumulative measured flicker in node Y.

For a chosen interval when both furnaces are in operation 50 s ... 650 s, the flicker levels in nodes A, B and Y are shown in table 1.

**Table 1.** Measured flicker levels for interval 50...650 s.

	$P_{st}$ measurement	$P_{st}$ contribution in Y
Node A	1.35	0.46
Node B	1.19	0.57
Node Y	0.67	-

As can be seen from figure 4 and as is shown in table 1, the contribution of furnace B to flicker in node Y is larger.

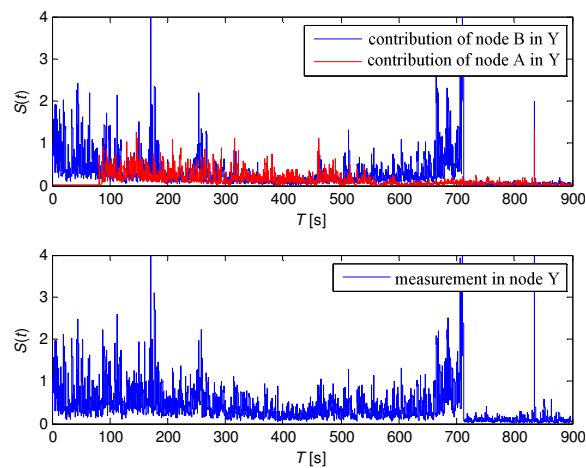


**Figure 4.** Contributions of flicker from nodes A and B in node Y and flicker measured in node Y.

Using the voltage measurements in nodes A and B and with  $NVTF$  factors from figures 2 and 3, the cumulative flicker in node Y can be obtained with (5). In this case the calculated flicker severity is  $P_{st,Y} = 0.70$ . The result is similar to the measured value of 0.67 from table 1.

**Approximation of flicker calculation with interharmonics**

The use of whole frequency spectrum shown in figures 2 and 3 is not necessary as the flickermeter response in [7] is defined only for the voltage fluctuations in the frequency range 0.5 – 40 Hz. Modulating frequencies around 8.8 Hz have the largest overall influence on flicker. In the case when only the frequencies of  $NVTF$  from figures 2 and 3 in the range 30 – 70 Hz would be used, the resulting flicker level in node Y would be 0.69. This is hardly a noticeable deviation from the previously obtained level of 0.70.

As can be seen from figures 2 and 3  $|NVTF|$  values for frequencies 30-70 Hz differ only slightly and can be set to the value at 50 Hz  $NVTF = |NVTF_{50Hz}|$ . Additionally in this range the phase angles can be approximated to 0 degrees. Therefore (6) can be used in which case we obtain

$P_{st,Y} = 0.71$ . This is again a relatively small deviation from the measured level in table 1.

**FLICKER PROPAGATION TO THE MV NETWORK**

Additional synchronised voltage measurements were conducted in the MV network as well. Figure 5 shows instantaneous flicker perception levels in both voltage levels in node Y measured during a particularly intense operation of furnace B in figure 1.

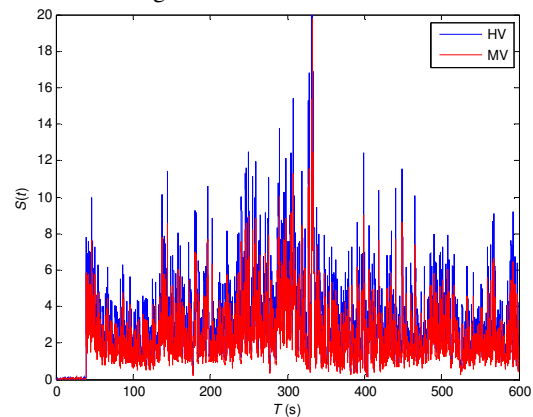


**Figure 5.** Synchronised instantaneous flicker levels in the HV and MV side of node Y.

Flicker levels calculated for the 10-minute interval in figure 5 are  $P_{st,HV} = 1.84$  and  $P_{st,MV} = 1.58$ . This means that the transfer factor between the HV and MV nodes is  $TF_{MV-HV} = 1.59/1.85 = 0.86$ . The square of this value is approximately equal to the ratio of instantaneous flicker perception levels in both nodes as shown in figure 6.

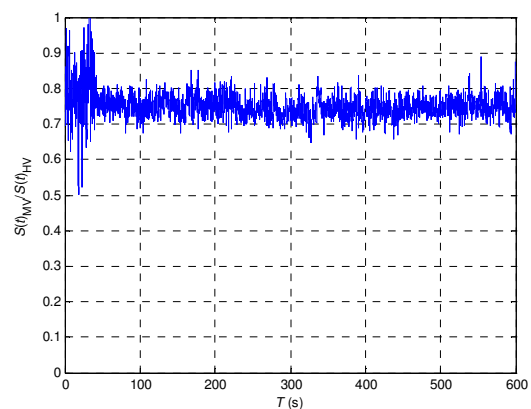


**Figure 6.** Ratio of instantaneous flicker levels from figure 5.

In system studies the damping between the HV and MV side is usually disregarded and  $TF_{MV-HV} \approx 1$ . The real transfer factor increases to this value in times of low load consumption. The calculated transfer factor between the HV

and MV node is shown in figure 7 for cases of expected high  $P_L = 22$  MW and low  $P_L = 5$  MW load consumption of the MV network.

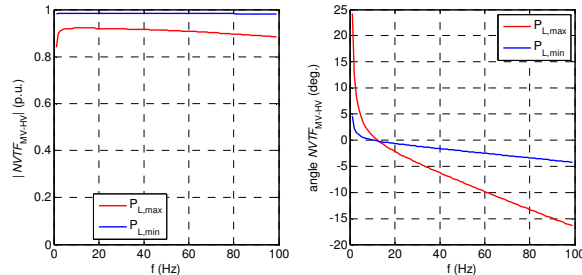


**Figure 7.** Calculated transfer factor between HV and MV node for high and low load consumption.

In the case of low load consumption (measurements in figure 5 were conducted during this time) the amplitude transfer factor in figure 7 equals approximately 0.98. This is higher than the previously determined factor of 0.86 and would give  $P_{st} = 1.80$  (as opposed to the measured  $P_{st} = 1.59$ ). This difference can be attributed to the fact that the dynamic nature of the load was not taken into account when determining the transfer factors in figure 7. Above all, motors with their mass inertia have a tendency to dampen voltage fluctuations and thus reduce flicker propagation from the HV to the LV grid. Consequently when studying the propagation of flicker from higher to lower voltage levels, one should also take the dynamic nature of the load into account to get a more accurate estimation of the flicker transfer factor.

## CONCLUSION

Propagation of voltage fluctuations and consequently flicker can be made with the method based on voltage interharmonics presented in this paper. The method can also be used for the summation of voltage fluctuations from several disturbing sources. The method is tested in a part of the Slovenian network influenced by two large arc furnaces. The method gives good results compared to flicker measurements. Additional calculations for flicker transfer from HV to MV grid are performed. The results show that the dynamic nature of the load should also be taken under account when determining voltage transfer factors.

## REFERENCES

- [1] B. Blažič, M.B. Kobav, et al., 2006, "Analysis of flicker levels in the Slovenian transmission network", *Electrotechnical review* 73(5), 291-296.
- [2] M. Maksić, I. Papič, 2011, "Analysis of flicker propagation with representative samples of network voltage", *IEEE Transactions on power delivery*. vol.

26, 2066-2067.

- [3] M. Maksić, I. Papič, 2010, "The calculation of flicker propagation in part of the Slovenian transmission network", *International Journal of Electrical Power and Energy Systems*. vol. 32, 1037-1048.
- [4] M. Maksić, B. Blažič, I. Papič, 2011, "Flicker summation coefficient in the Slovenian transmission network", *IEEE PowerTech*.
- [5] M. Maksić, I. Papič, 2010, "Calculation of flicker levels using voltage interharmonics", *IEEE Power and energy society general meeting 2010*.
- [6] S. Perera, D. Robinson, et al., 2006, "Synchronized flicker measurement for flicker transfer evaluation in power systems", *IEEE Transactions on power delivery*. vol. 21, 1477-1482.
- [7] *Standard IEC 61000-4-15: EMV - Testing and measuring techniques, Flickermeter - functional and design specifications*.
- [8] *Standard EN 50160: Voltage characteristics in public distribution networks*.